Use of residual waste glass in an alkali-activated binder – Structural characterization, environmental leaching behavior and comparison of reactivity

Abdelhadi Bouchikhi, Yannick Mamindy-Pajany, Walid Maherzi, Cyrille Albert-Mercier, Hamza El-Moueden, Mahfoud Benzerzour, Arne Peys, Nor-Edine Abriak

Version of Record: https://www.sciencedirect.com/science/article/pii/S2352710220335361
Manuscript_50596eac82533182c4bb0df4fb25deda

Use of residual waste glass in an alkali-activated binder – Structural characterization, environmental leaching behavior and comparison of reactivity

A. Bouchikhi[1*], Y. Mamindy-Pajany[1], W. Maherzi[1], C. Albert-Mercier[2], H. El-Moueden[1], M. Benzerzour[1], A. Peys[3], N. Abriak[1]

[1] IMT Lille-Douai, LGCgE-GCE, 941 rue Charles Bourseul, 59500 Douai, France
[2] LMCPA, Université Polytechnique des Hauts-de-France, Le Mont-Houy, 59313 Valenciennes.
[3] Sustainable Materials Management, VITO, Boeretang 200, 2400 Mol, Belgium

*Corresponding author; e-mail: abdelhadi.bouchikhi@imt-lille-douai.fr

Abstract:

Waste glass based geopolymers have a high potential in the future as an eco-friendly inorganic binder. However, limited studies are available on the use of the residue of waste glass recycling in this type of binder. This work investigates the valorization of Residual Waste Glass (RWG) (the final waste of glass recycling centers) crushed at d_{90} < 13 µm in a geopolymer activating solution. RWG is thus used as source of free silicon with metakaolin (MK) as source of aluminosilicates.. The activating solution from RWG was prepared in four ratios with a sodium hydroxide solution of 10M: R1 (10M-NaOH + 10g RWG), R2 (10M-NaOH + 20g RWG), R3 (10M-NaOH + 30g RWG) and R4 (10M-NaOH + 40g of RWG). The effect of these treatments on the mobility of metallic and metalloid trace elements (MMTE) and major elements (Si^{4+} and Al^{3+}) was measured. The structure of the solid phases produced after drying at 120°C/24h was studied using Fourier Transformed Infrared (FTIR) spectroscopy, Nuclear Magnetic Resonance (NMR) and XRD analyses. From these analyses, activating solution R3 was deemed optimal. The formulation of geopolymer mortars using MK and three activator sources: The optimized activating solution from RWG (R3), Commercial Sodium Silicate solution (CSS) and a reference activator formed by NaOH with RWG blended with the MK to obtain the same molar ratios in the geopolymer mixture. The mechanical and environmental performance results both highlight the interest of dissolving the RWG in NaOH first before insertion into the matrix. This study shows that treated glass R3 becomes an activating solution with good reactivity for obtaining a geopolymer binder and enhanced properties compared to the CSS source.

Keywords: Waste glass valorization; Geopolymer; Mechanical behavior; Environmental leaching performance

Highlights

- Sodium silicate solution can be produced from residual waste glass and NaOH
- 30 g of residual waste glass in 100 ml 10 M NaOH results in an optimal activator
- Better compressive strength properties for TGMK which reaches 28 MPa at 28 days

Graphical Abstract:

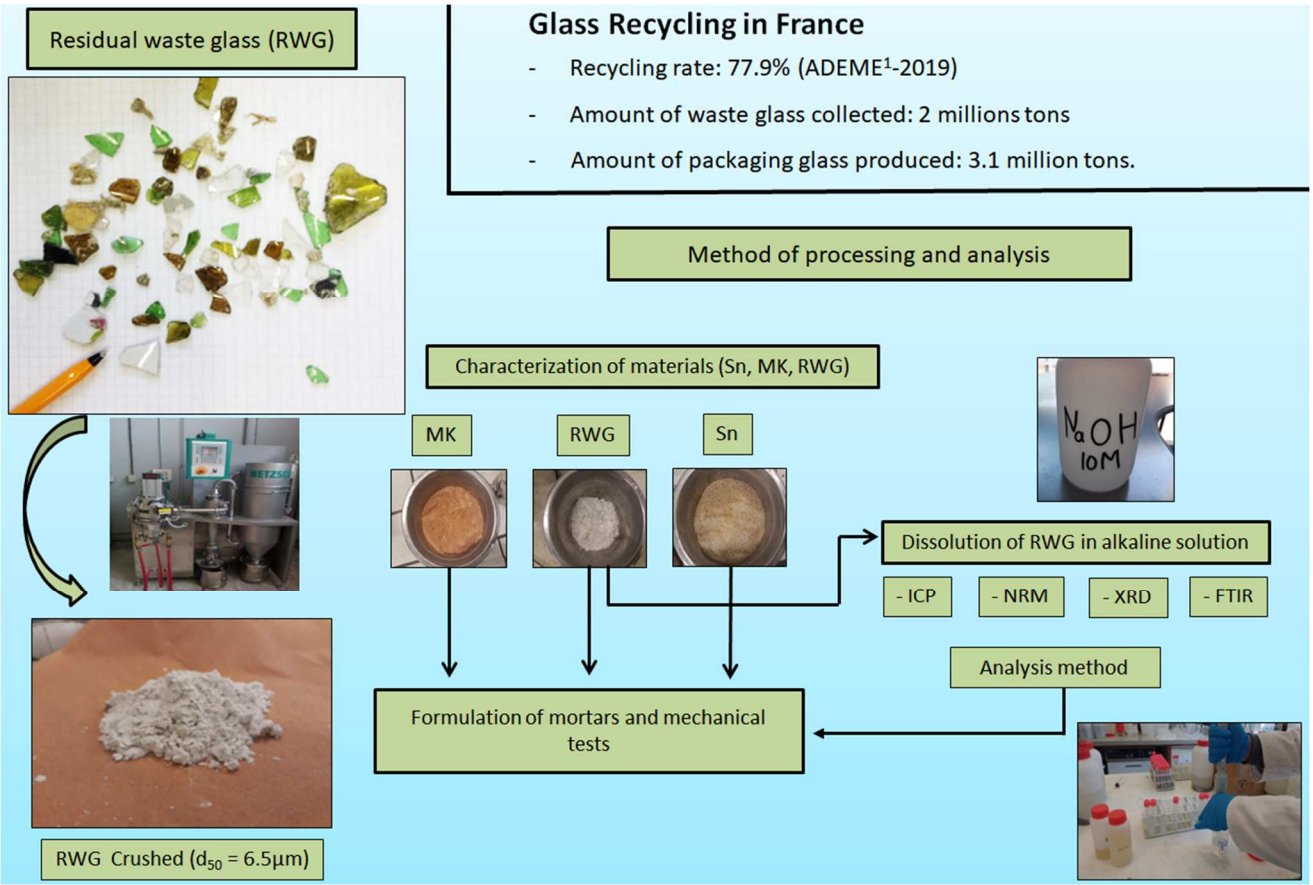

1 Introduction

Today's world faces many environmental challenges, among which it is not possible to ignore solid waste. Global statistics show that cities generated about 1.3 billion tons of solid waste in 2012. This quantity is expected to increase to 2.2 billion tons by 2025. An average city would have paid 205.4 billion dollars in 2012 for waste treatment, while the cost will be approximately 375.5 billion

[1] ADEME: Agence De l'environnement et de la maîtrise de l'énergie-France.

dollars in 2025 [1]. The production of Ordinary Portland Cement (OPC) requires a significant amount of energy with about 4200 kJ per ton of clinker, and 1.7 ton of natural resources such as limestone and clay used by cement factory. In addition, greenhouse gas emissions (mostly CO_2) are emitted: the cement industry produces between 6% and 7% of the global anthropogenic carbon dioxide emissions [2]. The formation of C_3S and C_2S at high temperature and the associated decarbonation of limestone are the main sources of CO_2 emissions[3,4].

The construction sector is one of the sectors which requires radical changes for future designs. The incorporation of waste into construction materials and the use of ecological binders are among the key aspects to improve this sector. Research pathways include geopolymer binders for which it is estimated that a replacement of Portland cement would reduce greenhouse gas emissions from <0 to ~80%, depending on the assumptions and mix-design [5–8]. Therefore, they have been studied intensively in the eco-environmental binder field. The number of scientific publications on the subject in 2017 reached more than 600 [9]. These inorganic binders are formed by mixing an alkaline silicate solution with an aluminosilicate powder precursor, such as natural resources, including calcined kaolinitic clays or coal fly ashes [10,11]. The production of this alkaline silicate solution represents the largest fraction of the environmental impact of the geopolymer binder [8]. It is thus important for the sustainability of geopolymer binders to find an alternative production route to obtain the alkaline activator.

In 1950, Glukhovsky was the first to propose the activation of aluminosilicates by alkaline compounds. Currently, there are several kinds of activators like NaOH, KOH, Na_2CO_3, K_2CO_3, Li_2CO_3, or alkaline silicate solutions ($Me_2O + nSiO_2$ with Me = Na, K or Li). These are salts formed by the reaction between soluble SiO_2 (silica) and alkaline hydroxides (Sodium (Na), Potassium (K), Lithium (Li)…). Alkaline silicates are known to be highly reactive and are characterized by their high water solubility. It is for this reason that they are called "water glasses" [12–17]

For geopolymer binders, several molar ratio intervals exist between Na_2O, Al_2O_3 and water. Davidovits and al [18,19], proposed molar ratios between the base elements to form geopolymer cement with properties equivalent to those of Ordinary Portland Cement (OPC):

$$0.2 < Na_2O / SiO_2 < 0.48$$
$$3.3 < SiO_2 / Al_2O_3 < 4.5$$
$$10 < H_2O / M_2O < 25$$
$$0.8 < Na_2O / Al_2O_3 < 1.6$$

The geopolymerization of aluminosilicates passes through five essential stages: dissolution, speciation equilibrium, gelation, reorganization and condensation [20]. These are steps related to the reaction mechanism of the aluminosilicates in solution. This is why several studies are interested in the release or leaching behavior of Al^{3+} and Si^{4+} ions in solution. These two elements are the formers of the geopolymer structure. The leaching of elements is mainly related to the alkalinity of the activator, the treatment temperature of calcination and the particle size of the aluminosilicate compounds studied. The degree of crystallization and the estimation of the amorphous components also give information on the mechanism of elements dissolution [21,22]. Lee and van Deventer [23] performed leaching at 20°C of fly ash in low or high alkalinity. Ca and Si were the first extracted elements, followed by Al in low alkaline media. The extraction of these elements increases in a solution with higher alkalinity. On the other hand, the formation of the geopolymer network was influenced by the process of dissolution [21]. Hajimohammadi and al. [24] investigated the mechanism of dissolution and nucleation of aluminosilicate particles. They explained that aluminate species facilitate the dissolution of Si^{4+} from the aluminosilicate precursor. Then, these dissolved elements will cause nucleation and polymerization in the supersaturated solution [24–26]. Other parameters also have an influence on the dissolution of these elements including the time of contact with the leaching medium and the liquid/solid ratio between the activating solution an aluminosilicate precursor. Among the most applied methods for studying the dissolution rate of aluminosilicate precursors, is that of Chen-Tan and al. [21] which consists of treating 5 g of material in an alkaline solution of 10M with a liquid/solid ratio of 10.

The chemical composition and amorphous structure of waste glass enable its use as sodium silicate source in geopolymerization [27,28]. The use of glass aggregates can improve the properties of the geopolymer matrix without pre-treatment. This improvement is linked to the ability of the glass aggregates to develop a gel-geopolymer at the interface as a function of time [27,29]. However, for an instantaneous reaction, a pre-treatment is necessary. Torres-Carrasco [17] proposed a method for dissolving the glass powder (with a particle size of d_{90} = 45 μm) in a 10M sodium hydroxide solution at 80 °C for 6 hours [30]. Waste glass consists of silica (which represents the basic element of its structure) and sodium or potassium (which exists in significant quantities in glass to reduce the melting temperature and viscosity of the melt) and is therefore a potential candidate for synthesis of the alkali-silicate activating solution. Several publications study the attack of waste glass in alkaline hydroxides with the aim to replace the marketed sodium silicate, which is the most expensive and least ecological part of a geopolymer [30–34]. In all these publications, the dissolution of a siliceous system is linked to the parameters mentioned before: particle size, alkalinity, time of contact. The dissolution rate of the glass also remains related to the temperature, which can be explained by the Arrhenius law of thermally activated reactions [11,35].

The optimization of the dissolution of RWG in sodium hydroxide and its impact on the mobility of metallic and metalloid trace elements (MMTE) is less studied. Similarly, the solid state products after drying the RWG-NaOH solution are rarely characterized. This study was focused on the optimization of the dissolution of RWG by quantification of the leaching of Si^{4+}, Al^{3+} and of the mobility of MMTE. This work also gives new experimental characterization insights of activated glass by means of characterization techniques like XRD, FTIR and NMR and SEM. After dissolution, optimized treated glass has been used as sodium silicate activating solution for a geopolymer binder. The compressive strength, open porosity and environmental stabilization of MMTE were studied in geopolymer mortars at different ages.

2 Materials and methods

2.1 Materials

Residual Waste Glass (RWG) contains impurities (such as porcelain) which cause a high melting temperature, making it difficult to employ it as raw material in the glass industry. This ultimate waste is collected in the region Hauts-de-France. The alkaline solution is prepared by dissolving NaOH pellets (purity 98.8%, provided by Hicher Scientific) in deionized water. For mechanical tests, mortars are made in a mixer according to NF EN 196-6. The metakaolin (MK) used as aluminosilicate source is characterized by a Si/Al ratio = 6 and median diameter d_{50} = 10µm. The sand is certified according to CEN 196-1 ISO standard. The particle size distribution is determined by sieving according to the requirements of NF EN 196-1. This sand is selected as the reference aggregate for standardized 4x4x16 cm^3 mortars.

2.2 Characterization methods

Physical properties were determined such as: the specific surface area was obtained by the Brunauer-Emmett-Teller (BET) calculation from nitrogen sorption experiments using an AGITENT Analyzer apparatus from Micromeritics (3FLEX Surface Characterization). Prior to analysis the samples were degassed with a Smart Prep degasser (VacPrep 061) to remove adsorbed contaminants and humidity. The specific density was measured using a Micromeritics ACCUPYC 1330 Helium Pycnometer. Particle size distribution was determined with laser diffraction Coulter LS12330 (ISO 13320-1). Porosity was measured by absorption of water under vacuum (pressure 25 mbar until saturation) for an initially dried sample of mass (M_d). The wet mass of the sample saturated with water was noted (M_e) and the mass measured during immersion of the sample in water was noted (M_e'). The expression of the porosity accessible to water, noted P (%), is given according to the equation Eq.1. The microscopic observations were conducted using scanning electron microscope (SEM) type Hitachi S-4300SE/N. Local chemical analysis was conducted using Energy Dispersive X-ray Spectrometer (EDS) with a Thermo Scientific Ultra Dry EDS detector coupled with the SEM.

$$Pw(\%) = \frac{Me-Md}{Me-Me'} \quad \text{Eq. 1}$$

Chemical analysis was performed using X-ray fluorescence analysis (XRF) with a S4-PIONEER equipped by a 4-kW generator and an anode in Rhodium. Mineralogical analysis was conducted using X-ray diffraction analysis (XRD) using a D8 Focus diffractometer from Bruker with an anode in cobalt ($\lambda K\alpha_1$ = 1.74 Å) equipped with a Lynx Eye detector. A fixed divergence slit of 0.2 mm was used. Measurements were taken from 5 to 80° with a step size of 0.02° and a time step of 1s. Data was collected at 40 kV and 30 mA. Fourier transformed infrared (FTIR) spectroscopy was carried out in transmittance mode in the mid-IR (MIR) region. Samples of 2 mg were dispersed in 200 mg of KBr and pressed to pellets of 13 mm diameter using a mechanical hand press. Measurements were performed using a Bruker IFS 66V FTIR spectrometer equipped with IR source. For each sample, 200 scans in the 400-4000 cm^{-1} (MIR) spectral range were recorded with a resolution of 2 cm^{-1}. A spectrum of the atmosphere was recorded for background correction. ^{29}Si MAS NMR spectra were recorded at a Larmor frequency of 79.5 MHz using a Bruker Avance 400 MHz (9.4 T) spectrometer. For the residual waste glass (RWG), the spectrum was obtained with 1152 scans with a pulse length of 5 µs (π/2) and a relaxation delay of 60 s (this time was optimized). For the treated glass (TG) and commercial sodium silicate (CSS), the spectrum was obtained with 1024 scans with a pulse length of 5 µs (π/2) and a relaxation delay of 10 s. The samples were spun at the magic angle of 54.7° and at spin rates of 5 kHz in 7 mm outer diameter zirconia rotors, with TMS (tetramethylsilane) used as reference. Spectral deconvolution was performed with Dmfit software [36].

The mobility of metallic and metalloid trace elements (MMTE) and major elements were measured after specimens leaching using various liquid-to-solid ratios. Leachates were filtered through acetate syringe filter at 0.45 µm and acidified with 2% (v/v) HNO_3 commercial solution (63% by weight) before performing chemical analyses by an inductively coupled plasma optical emission spectrometer (ICP-OES 5100 Agilent Technologies). The detection limit (DL) for the ICP-AES is presented in each element by (mg/kg). Leaching limit values of Inert waste (IW) and non-

hazardous waste (NHW) given by Directive 1999/31/EC on the landfill of waste were used to check the conformity of materials. Batch leaching tests were conducted according to EN 12457-2 [37] on the granular fraction of 0-4 mm for a constant liquid/solid ratio = 10 L/kg and by using the equilibrium time of 24 h.

Mechanical tests were carried out on 4x4x16cm^3 prismatic specimens according to the standard NF EN 196-1 [38]. Curing times chosen to measure the compressive strength are 1, 7 and 28 days with a curing temperature of 60°C. The samples were kept in plastic bags. The apparatus used was an INSTRON press of 15 tons.

2.3 Experimental program

The program of activation in sodium hydroxide is based on the experimental program described in the literature. Specifically, a treatment temperature of 85 ± 2 °C was maintained during 4 hours [15]. The mixing was performed continuously during these 4 hours using an agitator with speed 70 rpm. The amount of RWG in the solution was optimized: Four treatments were considered in this work, taking into account different quantities of RWG in 100 ml of 10 M NaOH solution. Details on the preparation of these four solutions are given in Table 1.

After the alkaline attack, the concentration of ions in the filtered solutions was analysed by ICP-AES. The major chemical elements (Si and Al) and MMTE (such as As, Fe, Co, Mo, Ba) are respectively studied as factors influencing the geopolymerization [22] and environmental leaching performance.

Structural characterization such as XRD, FTIR spectroscopy and NMR was carried out on solids resulting from the various reactions after drying at 120 °C for 24 hours. The optimum solution is selected for further tests as the one that provides the most sodium silicates. This optimal solution will be called “treated glass (TG)”. Fig. 1 gives more details on the followed experimental procedure.

Table 1: Conditions of waste glass activation in an alkaline medium.

Sample name	RWG (g)	Water (mL)	[NaOH] (mol/L)	Temperature/time
R1	10	100	10	85°C/4h

R2	20	100	10	85°C/4h
R3	30	100	10	85°C/4h
R4	40	100	10	85°C/4h

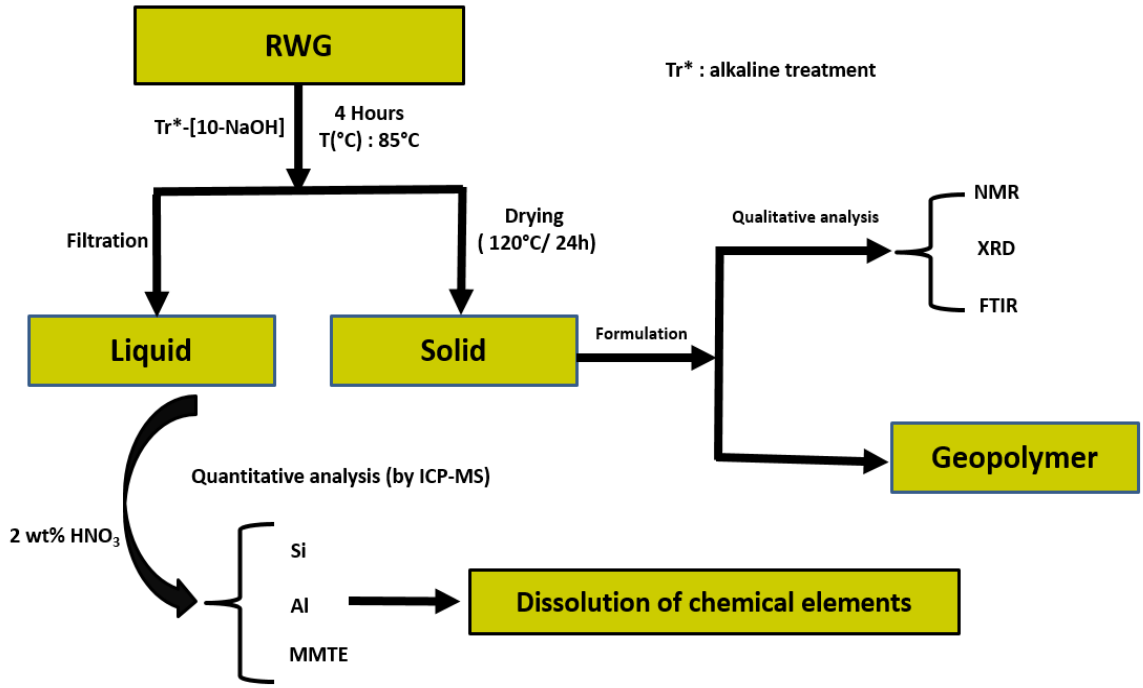

Fig. 1. Method of processing and analysis of RWG treated.

Mechanical tests are used to compare TG and CSS in a geopolymer matrix. An extra reference sample, RWG+NaOH, is added. In this sample, the RWG was mixed with the NaOH and MK without undergoing a pre-treatment. MK is used as aluminosilicate source in a constant amount in all mortars.

The mixture design of mortars based in amount of activator was set for an Ac: MK ratio = 0.22 (100 g of activator for 450 g of MK). NaOH was added in CSS and in RWG to maintain same molar concentration compared to mortar formed by GT activator. The Water: (Ac + MK) ratio is also fixed for 0.40 (250 g of water for 550 g of (Ac+KM)). The pH has been measured in the solutions after mixing each activator with water (1:10 ratio). Despite the fact that the RWG contains the same amount of sodium and alkaline earth elements (K^+, Ca^{2+}, Mg^{2+}) as TG [39], these elements are not immediately available to influence pH. The compositions of the mortars are given in Table 2. Formulations were made in 4x4x16 cm^3 prismatic moulds. The histogram presented in Fig. 2 gives an overview of the experimental approach for the mortar preparation. The exothermic effect is mainly linked to dissolution of the sodium silicate compounds in the TG. The hydration of the small amount

of Ca and Mg-containing compounds of the CaO and MgO types formed can also contribute to the dissolution heat of the preparation of TG [40].

Table 2: Composition of the geopolymer mortars.

Mortar	Formulation mass ratios			pH
	Sand/MK	A_c[2]/MK	Water/(A_c+MK)	
RMK	3	0.22	0.4	12.80
WGMK	3	0.22	0.4	12.57
TGMK	3	0.22	0.4	13.13

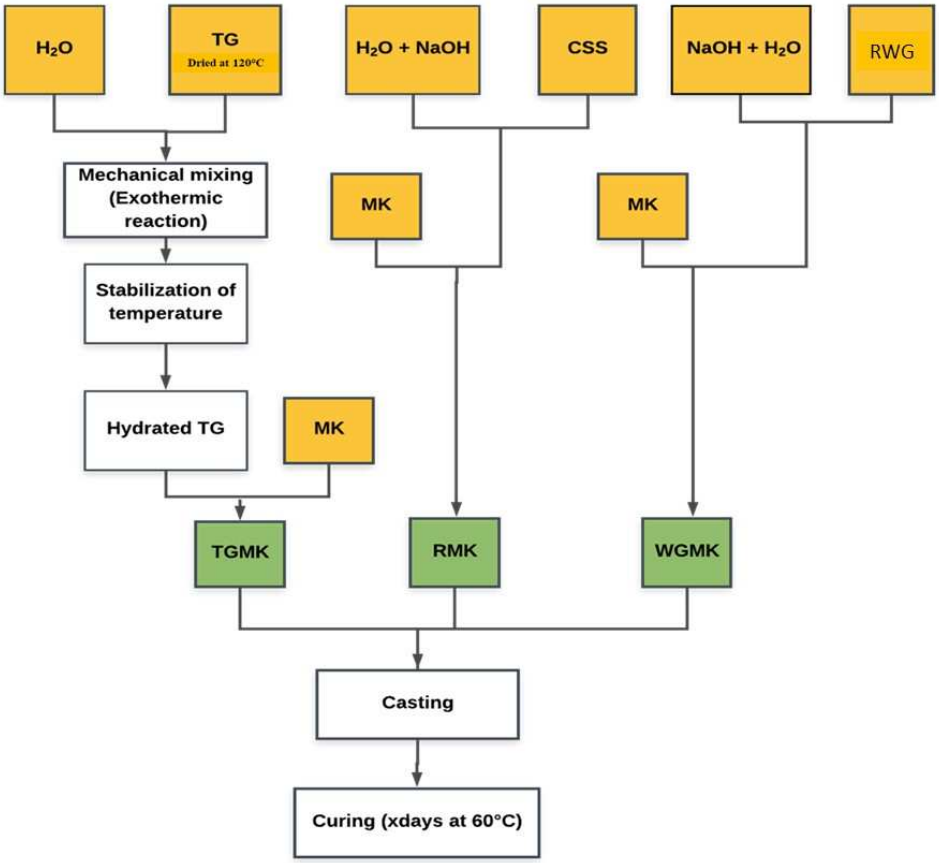

Fig. 2. Overview of mortar formulations and preparation procedures.

[2] A_c: Activators used in the mortars: CSS+NaOH, TG and WG+NaOH

3 Results and Discussion

3.1 Materials Characteristics

3.1.1 Particles size distribution

Glass is a non-porous and brittle material which explains that its outer surface represents the surface of contact with the outside environment. For this reason, the fineness of the glass plays a key role in its reactivity. Finer grain sizes result in higher reactivities. This relationship has been verified in several binder systems such as supplementary cementitious materials for blended cements and alkali-activated materials [41–43]. Specifically in geopolymerization, fineness of the precursor has been identified multiple times as key factor in the kinetics of the reactions [30,44,45]. The RWG was crushed using an air jet mill (NETZSCH-2015) and the grinding parameters were optimized in order to reach the target size of d_{50} = 6.5 µm and d_{90} =13 µm. For MK, the particle size is characterized by d_{50} = 7 µm and d_{90} = 48 µm. The particle size distribution of the sand (Sn) can be described by d_{50} = 500 µm and d_{90} = 2000 µm. Fig. 3 gives the granular distributions of these materials.

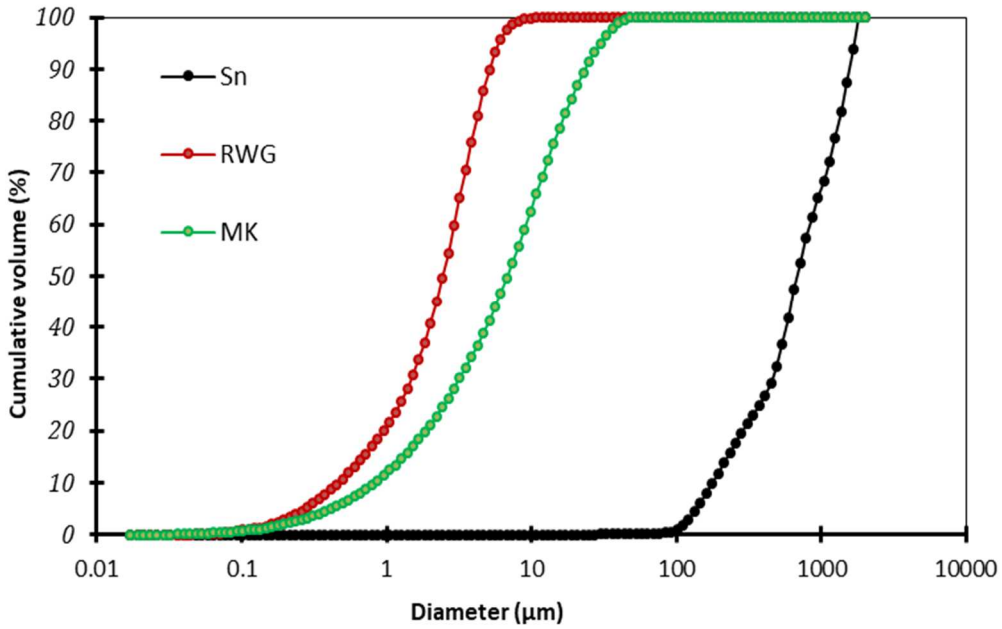

Fig. 3. Granular distributions of Sn, RWG and MK

3.1.2 Mineralogical and chemical characterization of materials

Table 3 illustrates the results of the chemical characterization of RWG and MK in molar percentage. RWG sample contains mainly 71% of SiO_2, 13% Na_2O and 12% of CaO. Minor elements

were aluminium (Al) (1%), chromium (Cr) (0.6%) and iron (Fe) (0.2%). On the other hand, MK contains SiO_2 and Al_2O_3 as major elements in its structure with 74% and 13% respectively. The XRD analysis on RWG, presented in Fig. 4-(A), shows that the majority of materials is an amorphous phase with some crystallization peaks. Some peaks present in XRD spectra are characteristic of the presence of quartz, calcite and magnesium silicate ($MgSiO_3$) compound. The SEM observation (insert of Fig. 4) gives the morphology of RWG aggregates before treatment. The MAS NMR^{29}Si spectra of the RWG in Fig. 4-(B) illustrate that the samples of glass are composed approximately of 30% of Q^4 and 70% of Q^3. This result remains coherent with soda-lime glasses and literature [46].

Table 3: Physical and chemical characterizations of RWG and MK.

Oxide (mol%)	**RWG**	**MK**
Na_2O	13.18	trace
MgO	1.76	0.42
Al_2O_3	0.95	13.23
SiO_2	71.07	73.95
K_2O	0.44	0.13
Fe_2O_3	0.15	0.37
CaO	12.38	1.36
Cr_2O_3	0.06	0
P_2O_5	trace	trace
SO_3	trace	trace
TiO_2	trace	0.82
L.O.I	0.2	0.7
Fire loss (550°C) (%)	0.1	1.2
Total Carbon (%)	0.07	0.60
Absolute density (g/cm^3)	2.54	2.62
Median diameter d_{50} (µm)	2.5	10
Specific surface BET (m²/kg)	792.6	500.6

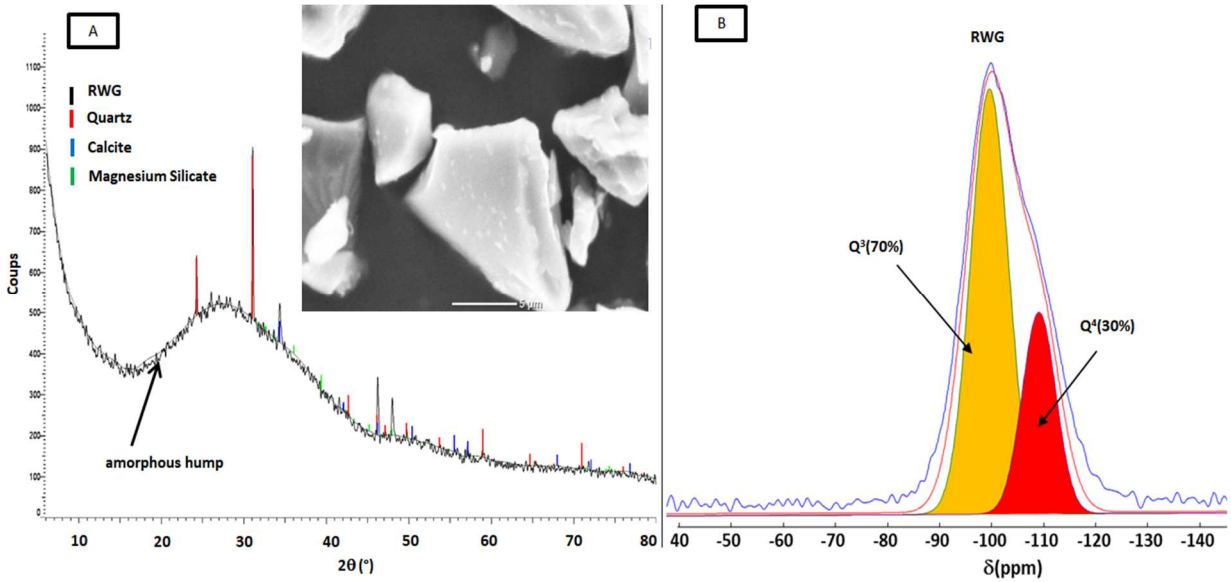

Fig. 4. (A) Diffractogram and (B) MAS NMR ^{29}Si spectra of RWG (in red: simulated spectra / in blue: experimental spectra).

3.2 Characterization of alkali activated waste glass

The dissolution of RWG is presented in Fig. 5 as the evolution of the quantity of major elements (Si, Al, Ca, and Mg) as a function of the amount of RWG added to the NaOH solution. Concerning the release of Si and Al, the analyzed quantity of these two elements increases as a function of the quantity of RWG in solution. A large amount of Si and Al is leached in the R3 and R4 treatments. The dissolution of Si and Al leads to the apparition of anionic charges (due to the breakage of bridging oxygens (BO)), which requires cationic charges to stabilize the system. This is the role of species such as Na^+, Ca^{2+}, K^+, etc., also present in solution. The phenomenon of dissolution explains the increase of free Si and Al.

The graphical representation of $n(SiO_2)/n(NaOH)$ ($n(SiO_2$ represents the amount of mole of SiO_2 that is released from RWG after dissolution in the NaOH solution) as a function of the quantity of Si and Al in solution (Fig. 6) shows that the increase of the amount of added RWG from 30 g to 40 g/100 ml (R3 to R4) has lower impact on the amount of Si and Al released. The amount of Si is stabilized at about 12 g/100 ml and 0.3 g/100 ml for Al, which explains that the alkaline solution is saturated in Si and Al between R3 and R4 or that the increase in $n(SiO_2)/n(NaOH)$ resulted in a

sufficient pH drop to stop further dissolution of the RWG. The saturation of media is also related to the thermodynamic equilibrium of the reaction medium and the ionic charge in solution.

The mobility of MMTE is important from an environmental point of view. The results presented in Table 4 show that the alkaline attack on the RWG structure leads to considerable release of MMTE compared to a control RWG sample without treatment (test according to standard NF EN 12457 [37]). A comparison between the different treatments R1-R4 shows an increase of the quantity of leachable MMTE, especially the elements Fe, As, Ba, Cr, Zn, Se, Pb, Sb, and Mo. An IW classification is given by the French Directive n°0289 published in 2014 [47]. This allows concluding that the release of some elements surpasses the values set in regulations. However, it is necessary to study the mobilization of these MMTEs in the geopolymer matrix after mixing with metakaolin in order to validate the environmental acceptability according to the French Directive.

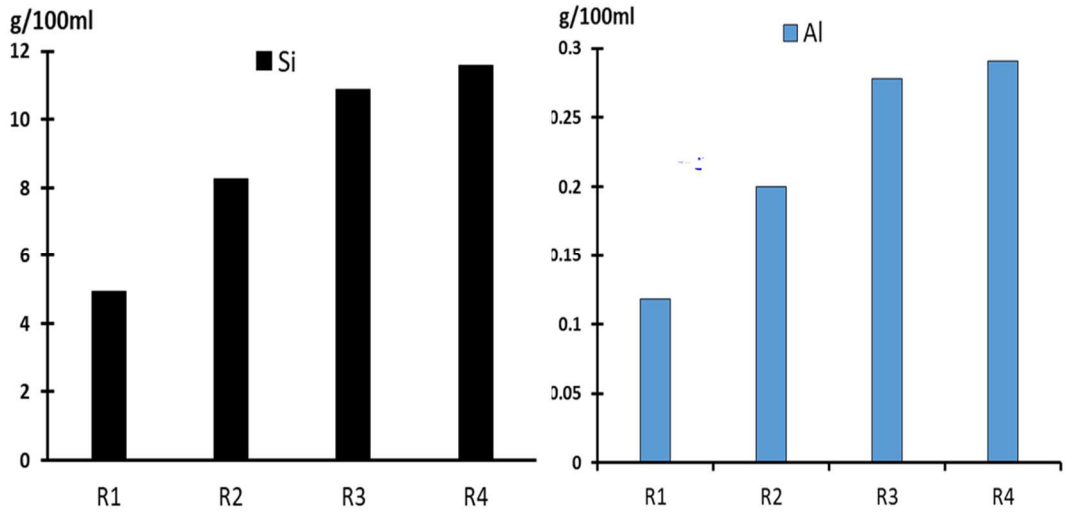

Fig. 5. Quantity of major elements analyzed in solution.

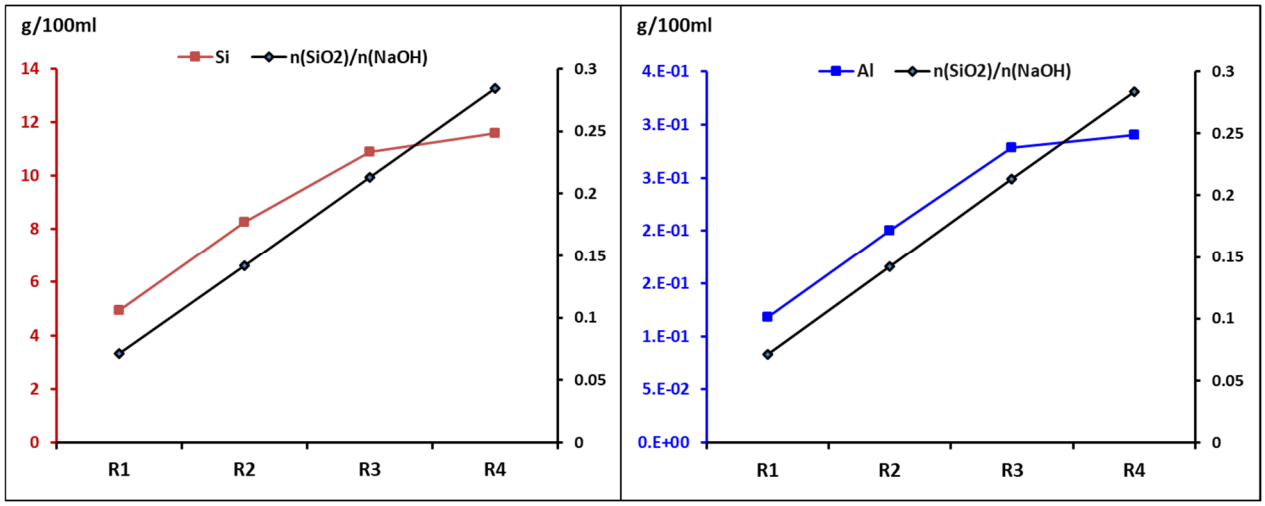

Fig. 6. Leaching of Si and Al as a function of molar ratio of n(SiO_2)/n(NaOH).

Table 4: Trace elements leached before and after alkaline treatment.

	Concentration (mg/Kg)										
Samples	As	Ba	Cd	Cr	Cu	Mo	Ni	Pb	Sb	Se	Zn
NaOH-10M	< 0.08	<0.06	< 0.01	< 0.03	<0.05	< 0.07	0.08	0.32	< 0.06	< 0.07	0.24
RWG-0M	0.56	7.20	0.01	0.07	<0.05	0.15	0.25	0.39	0.33	0.15	1.56
R1	1.00	9.12	0.03	0.14	<0.05	0.23	0.40	0.62	0.52	0.22	2.59
R2	1.38	6.97	0.04	0.60	<0.05	0.31	0.57	0.92	0.74	0.43	3.27
R3	1.27	3.21	0.04	0.64	<0.05	0.33	0.43	0.13	0.37	0.09	3.32
R4	< 0.08	<0.06	< 0.01	< 0.03	0.61	< 0.07	< 0.03	0.32	< 0.06	< 0.07	0.24
RSD	1.2	2.3	1.8	2.2	-	4.3	3.7	3.8	2.9	4.3	1.7
LD	0.08	0.06	0.01	0.03	0.05	0.07	0.03	0.03	0.06	0.07	0.06
IW	0.5	20	0.04	0.5	2	0.5	0.4	0.5	0.06	0.1	4
NHW	2	100	1	10	50	10	10	10	0.7	0.5	50

3.2.1 FTIR Analysis

In Fig. 7, the FTIR spectra of the RWG before treatment with NaOH only shows bands related to the structure of glass, such as Si-O-Si and Si-O-Al bending and stretching vibrations. The bands related to stretching vibrations are located between 1300 and 900 cm^{-1}, which indicates a highly polymerized glass network [48]. The position of the bands associated with bending (~800 cm^{-1}) and

rocking (~450 cm^{-1}) vibrations are in agreement with the presence of a highly polymerized glass. This was expected from the high SiO_2 content of the RWG. After treatment with NaOH and drying at 120 °C, bands shift and some new bands appear. The bands caused by Si-O-Si and Si-O-Al vibrations shift due to the the dissolution of the glass and depolymerization of the network by the Na^+ ions and thus an increase in Si-NBO (non bridging oxygen) linkages. This shift is most apparent for the stretching vibrations, for which the band evolves towards lower wavenumbers, and bending vibrations, for which the band flattens and disappears. This is commonly observed in silicate glasses [48,49]. New bands appearing in the spectra of the treated samples have varying intensities from one sample to another. Bands at 1450 and 870 cm^{-1} indicate the vibration of C-O bonds, originating from carbonates [50,51]. The Na or Ca in the treated RWG can have partially reacted with CO_2 in the air to produce Na- or Ca-carbonate phases. The bands at 1650 °C suggest the occurrence of O-H vibrations and thus indicate the presence of water [52,53]. A wide band between 3000 and 3500 cm^{-1} was observed confirming this (not presented in the figure). These bands reveal the presence of a large amount of adsorbed water, which indicates a strong retention of the water molecules by the formed phases.

According to the mechanism of Poole and al. [54], the presence of $Ca(OH)_2$ in the reaction medium influences the mechanism of attack of glass silica and alumina. The calcium hydroxide dissolved in the solution plays both the role of an hydroxide ion, replacing Na^+ consumed in the reactions, but also acts in the reactions to form products of alkali-silica reactions as following:

$$Ca(OH)_2 \rightarrow Ca^{2+} + 2OH^- \qquad \text{Eq.1}$$

$$2Si_{5/2}Na + Ca^{2+} \rightarrow Ca(SiO_{5/2})_2 + 2Na^+ \qquad \text{Eq.2}$$

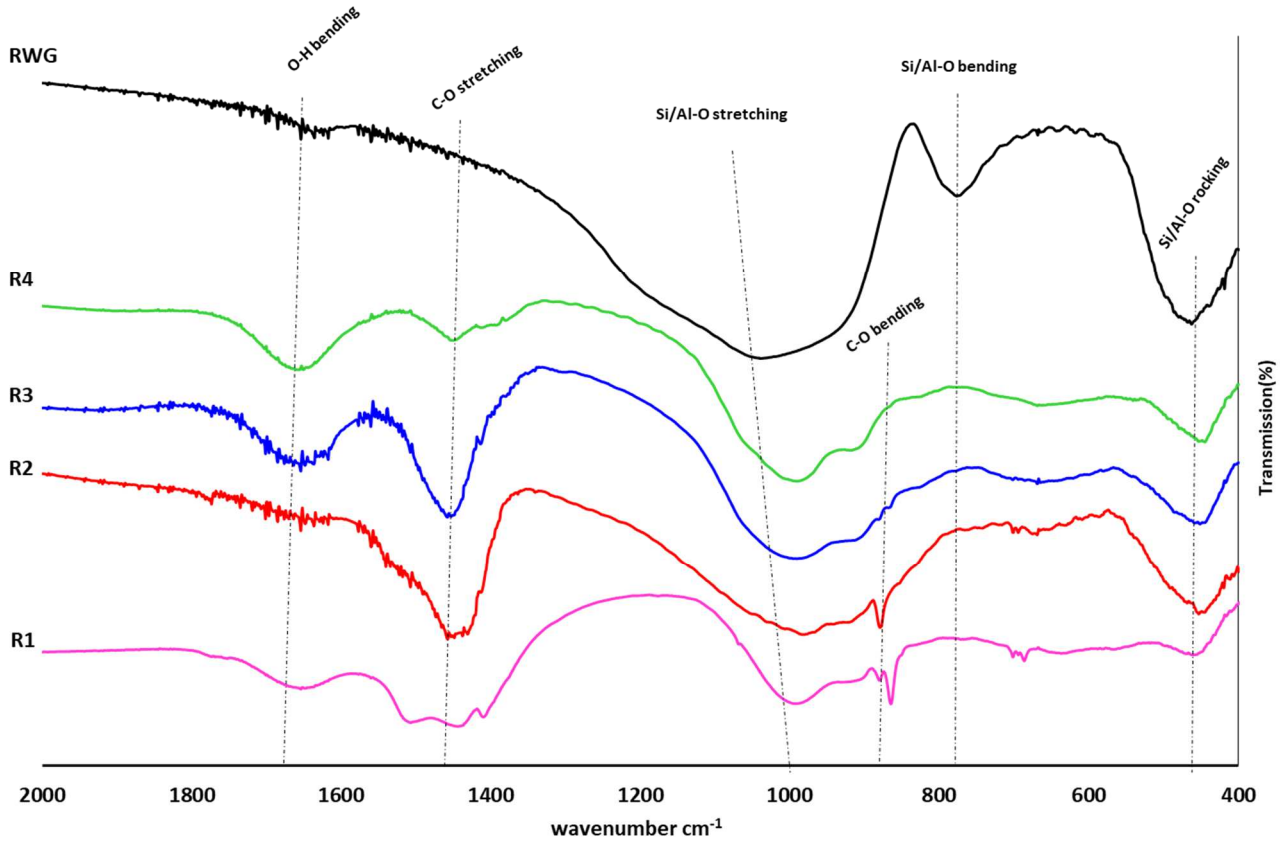

Fig. 7. Infrared spectra on samples analysed of RWG, R1, R2, R3 and R4.

3.2.2 XRD Analysis

In comparison with the initial state of the RWG, which presented itself as a highly amorphous structure, XRD results of the treated samples R1, R2, R3 and R4 in Fig. 8, show the presence of peaks characteristic for the dissolution of a glass structure. Sodium silicate (Na_2SiO_3) is the major phase present in all the treated glasses (from R1 to R4). There are also compounds containing Na, Ca, Al and Si like sodium calcium hydrogen silicate $NaCaHSiO_4$, Chabazite-Ca: $CaAl_2Si_4O_{12}$. In parallel, Na_2CO_3 is also very present in R1 and R2 because the amount of NaOH/RWG is higher. Other phases have been observed such as Chabazite silicate zeolitic products which include Chabazite-Ca ($CaAl_2Si_4O_{12}.6H_2O$), Chabazite-Na ($NaAlSi_2O_6.3H_2O$), Chabazite-Na, syn ($NaAlSiO_4.xH_2O$) and Chabazite-K, syn ($KAlSiO_4.xH_2O$). No quartz peaks are observed and the amorphous hump is not apparent in the diffractograms, indicating the high capacity of the NaOH solution to dissolve the glass structure and release the cations (Ca^{2+}, Mg^{2+}, K^+, Na^+) as well as anions (SiO_4^{4-}, AlO_4^{5-}) to form (M_2/NO)-$Al_2O_3.xSiO_2.yH_2O$ structures after precipitation, with N a monovalent cation, M a bivalent

cation, x varying from 2 to 10, y varying from 2 to 7 and Al_2O_3 and SiO_2 are framed cationic structures (framework) with oxygen [55]. In return, when the solution has a low $n(SiO_2)/n(NaOH)$ ratio, as is the case in R1 and R2, Na_2CO_3 products appear in the medium. These are a result of carbonation of the excess sodium during or after drying. XRD analyses show that for an optimal activator from RWG, it is necessary to use NaOH to dissolve the glass structure with a sufficiently high addition of RWG, in order to avoid the formation of sodium carbonate Na_2CO_3. The product of interest for this study is sodium silicate (Na_2SiO_3) in high amount. A high dosage of RWG as in the case of the R4 medium leads to residual unreacted RWG. The SEM observations in Fig. 8 underline a complete dissolution of the RWG in R1 due to the excess of NaOH. Therefore, treatment R3 is selected as an ideal mix for preparing an activator from the RWG. The analyses in the continuation of this paper were carried out only on the activator prepared by treatment R3. This activator is henceforth called "treated glass (TG)".

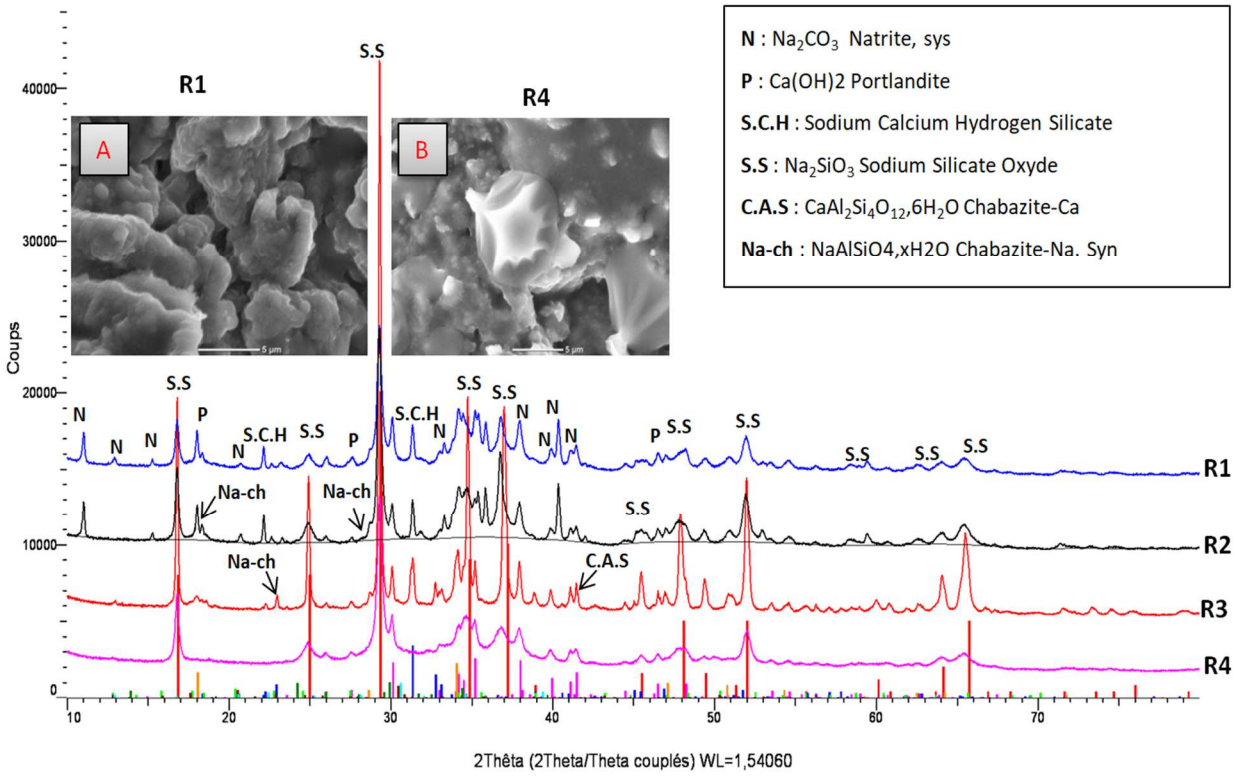

Fig. 8. XRD analyses on RWG treated by R1, R2, R3 and R4; (A): SEM image of R1 and (B): SEM image of R4.

3.2.3 ^{29}Si NMR analyses on RWG, TG and CSS

The ^{29}Si NMR analyses on RWG, TG (R3) and CSS (Fig. 9) show the contribution of the different resonances of ^{29}Si in all the samples. For RWG, NMR spectra allow to highlight three types of resonances: Q^4 around -110 ppm, Q^3 around -100 ppm and Q^2 around -90 ppm. Treatment of the NMR resonances peaks by Dmfit [36] highlights that the samples are composed of 30% Q^4 and 70% Q^3. This confirms the high degree of polymerization observed in the FTIR spectroscopy results. After treatment, the TG contains only Q^0 and Q^1 silicate species. ^{29}Si NMR analyses reveal the presence of 90% of ^{29}Si in Q^1 form and 10% of Q^0. NMR analyses on CSS reveal the presence of a strong resonance peak at -70 and -90 ppm, which is related to the presence of Q^2 (46%) and Q^1 (41%) species; the Q^0 represent 13%. For comparison, if the activator contains more Q^0 and Q^1, its reactivity is higher. This suggests that the reactivity of the TG might be higher than that of the CSS.

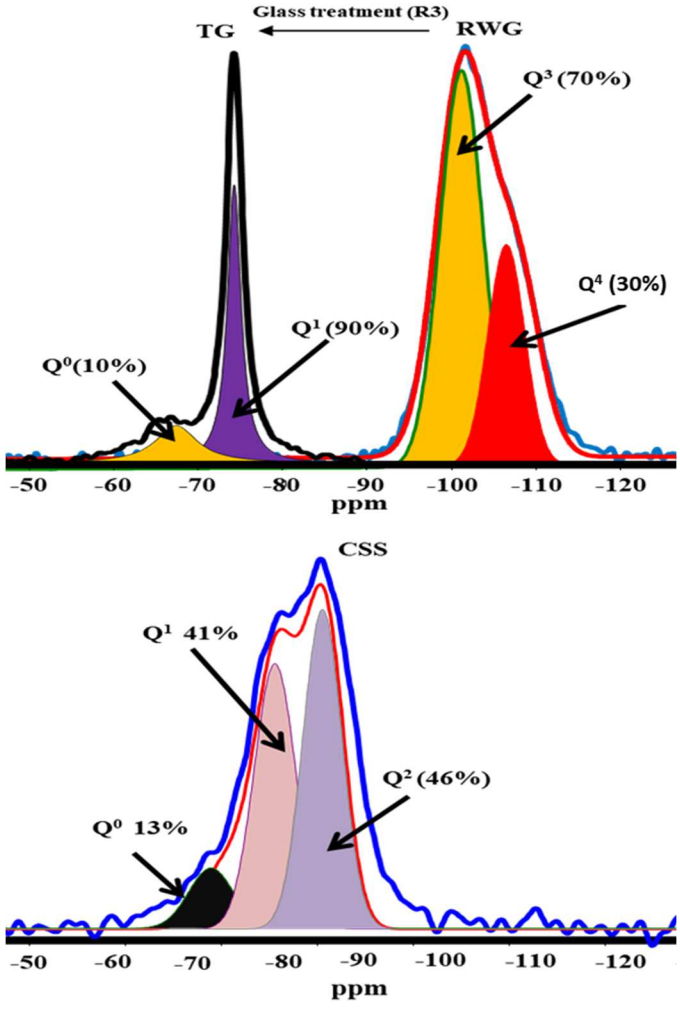

Fig. 9. ^{29}Si NMR analyses on a) RWG, b) TG and c) CSS (in red: simulated spectra / in blue: experimental spectra).

3.3 Mechanical and environmental results

The mechanical evolution presented in Fig. 10 highlights a compressive strength for TGMK around 30, 35 and 36 MPa for respectively 1, 7 and 28 days of curing at 60 °C. On other hand, the compressive strength for RMK increases from 2 MPa at 1 day of curing to 7 MPa at 28 days of curing, and from 4 to 5 MPa (for same time of curing) for WGMK. This comparison allows to reveal the high reactivity of TG compared to the CSS and WG formulations. The compressive strength is 5 times higher for TGMK after 7 days of curing compared to raw glass and 7 times higher compared to CSS. The activator from TG had a higher pH and contained more available silicon (Q^0 species), which promotes the formation of the binder phase and improves the mechanical properties of the matrix. On the other hand, untreated glass does not have an extensive amount of active silicon, which explains that the mechanical properties remain low compared to the TGMK.

The evolution of the open porosity accessible to water as a function of the curing time of the mortars (Fig. 11) is compatible with the geopolymerization reactions, with a porosity around 18%, 17% and 16% respectively for RMK, WGMK and TGMK after 1 day of curing. The porosity is approximately 17%, 16% and 15% for the same samples after 28 days of curing. These values are coherent with other studies on geopolymer matrices in standard mortars [31]. The presence of other chemical elements such as Ca^{2+}, K^{+}, Mg^{2+} in hydrated forms influences the nature of the geopolymer network formed which could be explained by the relatively low porosity in TGMK compared to RMK and WGMK [20].

The small difference between the porosity accessible to water in all the samples and, on the contrary, the high difference of compressive strength values indicates that another parameter should be looked at to explain the strength results. The water absorption results show a similar compactness or macroporosity in the different mortars. Therefore, it is rather the inherent strength of the binder than the pore structure that defines the strength of the studied geopolymer mortars. This is most probably a chemical effect that has an impact on the solidification of the geopolymer matrix, associated with the higher pH and higher amount of silicate species with a lower connectivity. .

The environmental leaching results show a stabilization of the MMTE (Table 5) with values lower than those set in IW classification, with the exception of Selenium (Se) and Arsenic (As) which remain around 0.12 and 0.8 respectively. However, the values do not exceed the NHW classification [47]. This stabilization is linked to the nature of the polymeric network in a geopolymer binder, characterized by a strong capacity to immobilize different types of pollutants, in particular MMTE [56–58]. The existence of MK and zeolitic compounds (resulting from the activation of glass) in the medium gives a strong cation exchange capacity characterized by the release of (K^+, Ca^{2+}, Na^+, Mg^{2+}) and the binding of MMTE on the negative surface of Al and Si [59]. The amorphous zeolite-like structure of the geopolymer can act similarly [60,61]. Furthermore, other types of immobilization in the gel-geopolymer networks are physical immobilization by an encapsulation of the large MMTE ions in the pores of the geopolymer network.

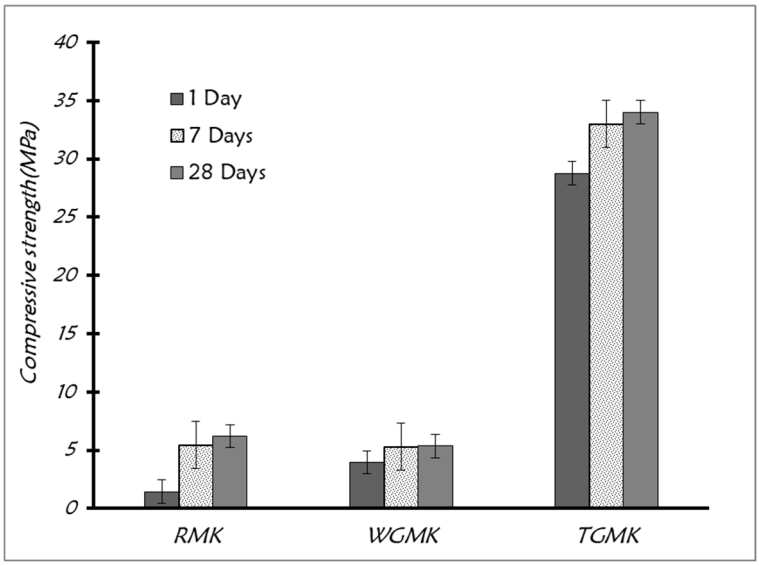

Fig. 10. Mechanical properties of mortars.

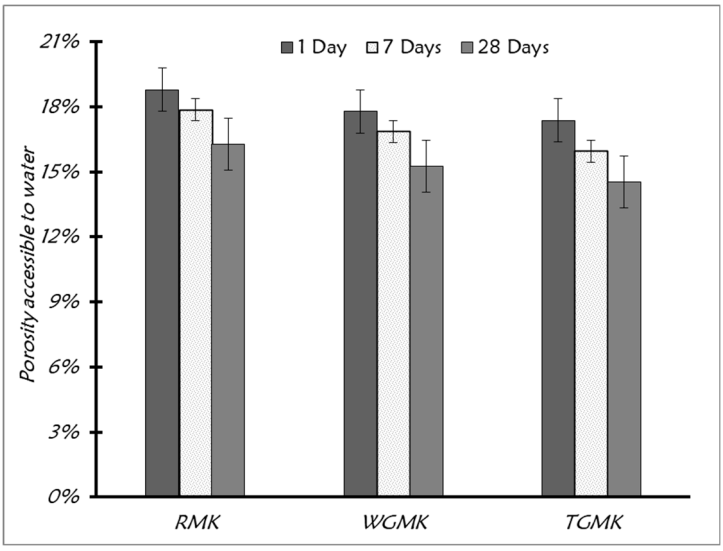

Fig. 11. Porosity measured by water absorption.

Table 5: Mobility of MMTE in the mortars study TGMK, RMK and WGMK

	As	*Ba*	*Cd*	*Cr*	*Cu*	*Mo*	*Ni*	*Pb*	*Sb*	*Se*	*Zn*
TGMK	0.8	<0.06	<0.01	0.06	<0.05	0.098	<0.03	<0.03	<0.06	0.12	< 0.06
RMK	0.72	<0.06	< 0.01	0.08	1.3	<0.07	0.15	<0.03	0.15	0.21	1.5
WGMK	0.59	<0.06	0.02	0.05	0.04	0.12	0.37	<0.03	0.23	<0.07	0.15
MK	<0.08	<0.06	<0.01	0.41	<0.05	<0.07	<0.03	<0.03	0.13	<0.07	<0.06
RSD	1.2	2.3	1.8	2.2	-	4.3	3.7	3.8	2.9	4.3	1.7
LD	0.08	0.06	0.01	0.03	0.05	0.07	0.03	0.03	0.06	0.07	0.06
IW	0.5	20	0.04	0.5	2	0.5	0.4	0.5	0.06	0.1	4
NHW	2	100	1	10	50	10	10	10	0.7	0.5	50

3.4 Microstructure of the geopolymer mortars

The SEM observations were realized with the objective to study the morphology of the phases existing in the different mortars (TGMK, RMK and WGMK). The SEM observations and chemical analyzes realized by EDS were evaluated on two sections by sample. They show the presence of characteristic dominant phases in each formulation. (Fig. 12-(A- B-C and D) illustrates that the binders in these different mortars have different textures and different chemical compositions. The binder phases in TGMK (Fig. 12-A) have a denser texture than the binder in RMK,. TGMK, contains also a significant amount of other elements such as calcium (4.4 wt%) and magnesium (0.5 wt%). These components are capable to participate in the geopolymerization of Al and Si and influence the morphology of the binder [62]. Natrite Na_2CO_3 (N) is present in WGMK. As a consequence of the

remaining free NaOH, a large part of Na^+ reacts with carbon dioxide of air to form natrite (Fig. 13-A-B and C)) [20,62]. The presence of NaOH in excess did not give improvements of the mechanical properties of WGMK. Therefore, it is not interesting to use a large quantity of NaOH compared to the available Si and Al, which are considered as the basic elements to form the geopolymer network. On the other hand, sufficient NaOH is needed for the activation of Si and Al and to form the N-A-S-H network. Other phases (N,C)-A-S-H and C-S-H) [63] can also appear in the form of needles or as a continuous binder. Other parameters that can have influenced the morphology of binder phases are the curing conditions such as temperature, or the concentration of sodium hydroxide [64].

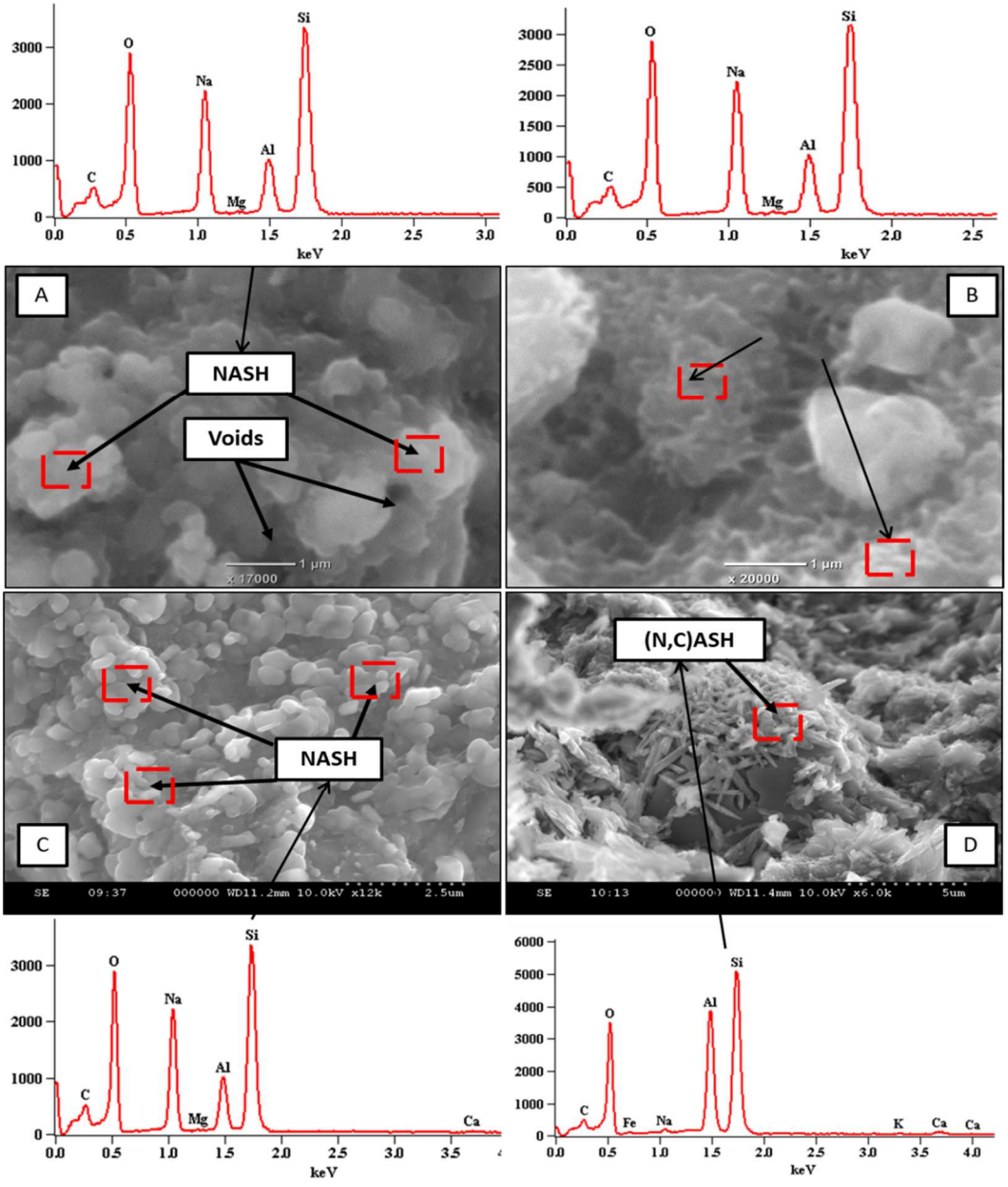

Fig. 12. SEM observations of the binder (A): RMK, (B): WGMK and (C) and (D): TGMK.

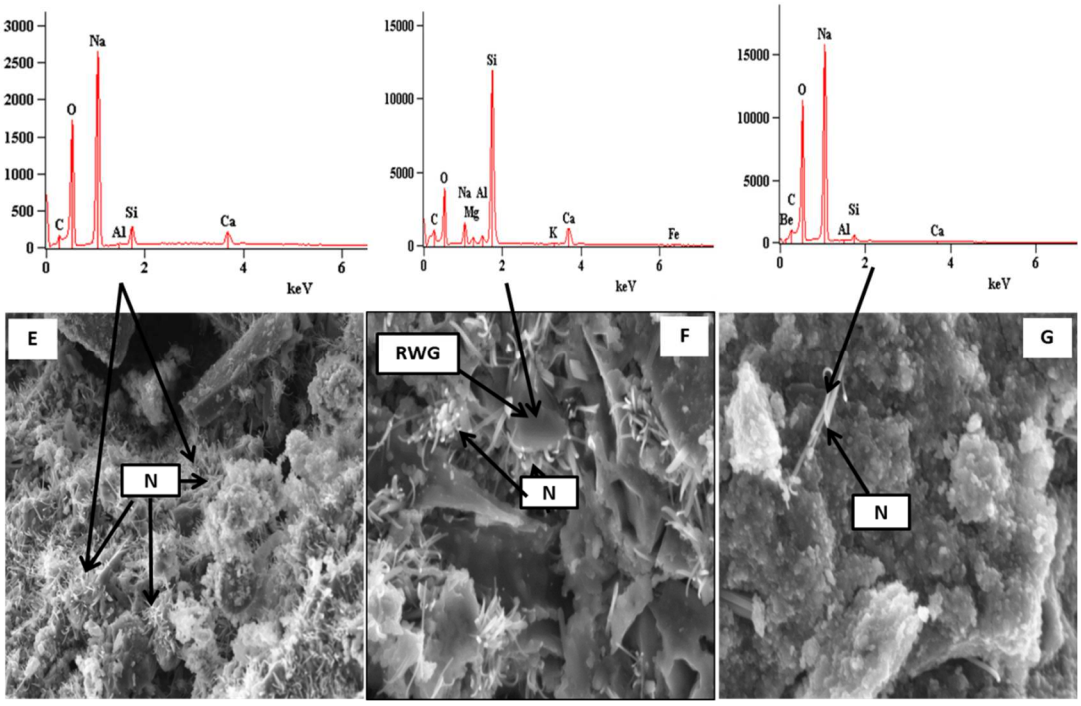

Fig. 13. SEM observations of (E): RMK, (F): WGMK and (G): TGMK.

4 Conclusion

This work provides information on the optimization of the treatment of residual waste glass (RWG) with NaOH to serve as activator for metakaolin-based geopolymers. The impact on the reactivity in a geopolymer binder and on the environmental leaching behavior of metallic and metalloid elements (MMTE) is assessed.

- To promote the dissolution of the glass structure in an alkaline medium, an optimization of the attack protocol was carried out. It allowed to activate 30 g of RWG (d_{90} <13 µm) in 100 ml of a 10 M-NaOH solution with an activation temperature set at 85°C for 4 hours.
- The activation of RWG by NaOH leads to the production of sodium silicate (Na_2SiO_3) as major phase, since the glass structure contains 72 mol% of silica. Other phases are also produced in a small percentage depending on the low amount of Ca, K, Mg, Al and Fe. Chabazite-Ca ($CaAl_2Si_4O_{12}.6H_2O$), Chabazite-Na ($NaAlSi_2O_6.3H_2O$), syn ($NaAlSiO_4.xH_2O$) and Chabazite-K, syn ($KAlSiO_4.xH_2O$) are some examples.
- The activation of RWG generates a significant mobilization of the MMTE, which requires checking their stabilization again in the proposed geopolymer formulations. In the studied case,

the MMTE are stabilized in the mortars, which can be explained by the retention capacity of these pollutants by the geopolymer matrix.

- The comparison between activators formed from the optimized treated RWG and a commercial sodium silicate (CSS) solution in geopolymer binders allows to conclude that the activator formed by the treated glass (TG) make these chemical compositions available for the formation of the geopolymer phases which leads to a great improvement of compressive strength compared to CSS.

Acknowledgements

Authors gratefully acknowledge the useful contribution of Bertrand Revel (Centre Commun de Mesures RMN—Université de Lille), and the Water Agency (Agence de l'eau des Hauts-de-France) who has financed this study. This work was realized in the laboratory of civil engineering department of IMT Lille Douai.

References:

[1] D. Hoornweg, P. Bhada, What a Waste. A Global Review of Solid Waste Management, Urban Dev. Ser. Knowl. Pap. 281 (2012) 44 p. doi:10.1111/febs.13058.

[2] K.L. Scrivener, R.J. Kirkpatrick, Innovation in use and research on cementitious material, Cem. Concr. Res. 38 (2008) 128–136. doi:10.1016/j.cemconres.2007.09.025.

[3] G. Habert, J.B. D'Espinose De Lacaillerie, N. Roussel, An environmental evaluation of geopolymer based concrete production: Reviewing current research trends, J. Clean. Prod. 19 (2011) 1229–1238. doi:10.1016/j.jclepro.2011.03.012.

[4] E. Benhelal, G. Zahedi, E. Shamsaei, A. Bahadori, Global strategies and potentials to curb CO2 emissions in cement industry, J. Clean. Prod. 51 (2013) 142–161. doi:10.1016/j.jclepro.2012.10.049.

[5] B.C. McLellan, R.P. Williams, J. Lay, A. Van Riessen, G.D. Corder, Costs and carbon emissions for geopolymer pastes in comparison to ordinary portland cement, J. Clean. Prod. 19 (2011) 1080–1090. doi:10.1016/j.jclepro.2011.02.010.

[6] G. Habert, C. Ouellet-Plamondon, Recent update on the environmental impact of geopolymers, RILEM Tech. Lett. 1 (2016) 17. doi:10.21809/rilemtechlett.v1.6.

[7] A. Mellado, C. Catalán, N. Bouzón, M. V. Borrachero, J.M. Monzó, J. Payá, Carbon footprint of geopolymeric mortar: Study of the contribution of the alkaline activating solution and assessment of an alternative route, RSC Adv. 4 (2014) 23846–23852. doi:10.1039/c4ra03375b.

[8] A. Peys, L. Arnout, B. Blanpain, H. Rahier, K. Van Acker, Y. Pontikes, Mix-design Parameters and Real-life Considerations in the Pursuit of Lower Environmental Impact Inorganic Polymers, Waste and Biomass Valorization. 9 (2018) 879–889. doi:10.1007/s12649-017-9877-1.

[9] J. Davidovits, Geopolymer Chemistry and Applications 5 th edition, 2015.

[10] K. tuo Wang, L. qiu Du, X. sen Lv, Y. He, X. min Cui, Preparation of drying powder inorganic polymer cement based on alkali-activated slag technology, Powder Technol. 312 (2017) 204–209. doi:10.1016/j.powtec.2017.02.036.

[11] R. Idir, M. Cyr, A. Pavoine, Investigations on the durability of alkali-activated recycled glass, Constr. Build. Mater. 236 (2020) 117477. doi:10.1016/j.conbuildmat.2019.117477.

[12] M. Torres-Carrasco, F. Puertas, Waste glass as a precursor in alkaline activation: Chemical process and hydration products, Constr. Build. Mater. (2017).

doi:10.1016/j.conbuildmat.2017.02.071.

[13] S. Tome, M.-A. Etoh, J. Etame, K. Sanjay, Characterization and Leachability Behaviour of Geopolymer Cement Synthesised from Municipal Solid Waste Incinerator Fly Ash and Volcanic Ash Blends, Recycling. 3 (2018) 50. doi:10.3390/recycling3040050.

[14] M. Criado, A. Fernández-Jiménez, A. Palomo, I. Sobrados, J. Sanz, Effect of the SiO2/Na2O ratio on the alkali activation of fly ash. Part II: 29Si MAS-NMR Survey, Microporous Mesoporous Mater. (2008). doi:10.1016/j.micromeso.2007.05.062.

[15] P. Duxson, A. Fernández-Jiménez, J.L. Provis, G.C. Lukey, A. Palomo, J.S.J. Van Deventer, Geopolymer technology: The current state of the art, J. Mater. Sci. 42 (2007) 2917–2933. doi:10.1007/s10853-006-0637-z.

[16] E.T. Bueno, J.M. Paris, K.A. Clavier, C. Spreadbury, C.C. Ferraro, T.G. Townsend, A review of ground waste glass as a supplementary cementitious material: A focus on alkali-silica reaction, J. Clean. Prod. 257 (2020) 120180. doi:10.1016/j.jclepro.2020.120180.

[17] M. Torres-carrasco, J.G. Palomo, F. Puertas, Sodium silicate solutions from dissolution of glass wastes . Statistical analysis, Mater. Construcción. 64 (2014) 1–14. doi:10.3989/mc.2014.05213.

[18] J. Davidovits, Geopolymers - Inorganic polymeric new materials, J. Therm. Anal. 37 (1991) 1633–1656. doi:10.1007/BF01912193.

[19] Z. Shi, C. Shi, S. Wan, Z. Zhang, Effects of alkali dosage and silicate modulus on alkali-silica reaction in alkali-activated slag mortars, Cem. Concr. Res. 111 (2018) 104–115. doi:10.1016/j.cemconres.2018.06.005.

[20] P. Duxson, A. Fernández-Jiménez, J.L. Provis, G.C. Lukey, A. Palomo, J.S.J. Van Deventer, Geopolymer technology: The current state of the art, J. Mater. Sci. 42 (2007) 2917–2933. doi:10.1007/s10853-006-0637-z.

[21] N.W. Chen-Tan, A. Van Riessen, C. V. Ly, D.C. Southam, Determining the reactivity of a fly ash for production of geopolymer, J. Am. Ceram. Soc. 92 (2009) 881–887. doi:10.1111/j.1551-2916.2009.02948.x.

[22] C. Weeks, R.J. Hand, J.H. Sharp, Retardation of cement hydration caused by heavy metals present in ISF slag used as aggregate, Cem. Concr. Compos. 30 (2008) 970–978. doi:10.1016/j.cemconcomp.2008.07.005.

[23] W.K.W. Lee, J.S.J. Van Deventer, Structural reorganisation of class F fly ash in alkaline

silicate solutions, Colloids Surfaces A Physicochem. Eng. Asp. 211 (2002) 49–66. doi:10.1016/S0927-7757(02)00237-6.

[24] A. Hajimohammadi, J.S.J. van Deventer, Dissolution behaviour of source materials for synthesis of geopolymer binders: A kinetic approach, Int. J. Miner. Process. 153 (2015) 80–86. doi:10.1016/j.minpro.2016.05.014.

[25] A. Hajimohammadi, J.L. Provis, J.S.J. van Deventer, Effect of Alumina Release Rate on the Mechanism of Geopolymer Gel Formation, Chem. Mater. 22 (2010) 5199–5208. doi:10.1021/cm101151n.

[26] H.A. Gasteiger, W.J. Frederick, R.C. Streisel, Solubility of aluminosilicates in alkaline solutions and a thermodynamic equilibrium model, Ind. Eng. Chem. Res. 31 (1992) 1183–1190. doi:10.1021/ie00004a031.

[27] N. Toniolo, A. Rincón, J.A. Roether, P. Ercole, E. Bernardo, A.R. Boccaccini, Extensive reuse of soda-lime waste glass in fly ash-based geopolymers, Constr. Build. Mater. 188 (2018) 1077–1084. doi:10.1016/j.conbuildmat.2018.08.096.

[28] A. Hajimohammadi, T. Ngo, J. Vongsvivut, Interfacial chemistry of a fly ash geopolymer and aggregates, J. Clean. Prod. 231 (2019) 980–989. doi:10.1016/j.jclepro.2019.05.249.

[29] A. Hajimohammadi, T. Ngo, A. Kashani, Glass waste versus sand as aggregates: The characteristics of the evolving geopolymer binders, J. Clean. Prod. 193 (2018) 593–603. doi:10.1016/j.jclepro.2018.05.086.

[30] M. Torres-Carrasco, F. Puertas, Waste glass in the geopolymer preparation. Mechanical and microstructural characterisation, J. Clean. Prod. 90 (2015) 397–408. doi:10.1016/j.jclepro.2014.11.074.

[31] M. Torres-carrasco, J.G. Palomo, F. Puertas, Sodium silicate solutions from dissolution of glass wastes. Statistical analysis, Mater. Construcción. 64 (2014) 1–14. doi:10.3989/mc.2014.05213.

[32] J.M. Rincon, M. Romero, C. Diaz, V. Balek, Z. Malek, Thermal behaviour of silica waste from a geothermal power station and derived silica ceramics, J. Therm. Anal. Calorim. 56 (1999) 1261–1269.

[33] M. Torres-Carrasco, F. Puertas, Waste glass as a precursor in alkaline activation: Chemical process and hydration products, Constr. Build. Mater. 139 (2017) 342–354. doi:10.1016/j.conbuildmat.2017.02.071.

[34] R. Vinai, M. Soutsos, Production of sodium silicate powder from waste glass cullet for alkali activation of alternative binders, Cem. Concr. Res. 116 (2019) 45–56. doi:10.1016/j.cemconres.2018.11.008.

[35] J. Grynberg, Mécanismes physiques et chimiques mis en jeu lors de la fusion du mélange SiO2-Na2CO3, PIERRE ET MARIE CURIE, 2013. https://tel.archives-ouvertes.fr/tel-00829455.

[36] D. Massiot, F. Fayon, M. Capron, I. King, L. Calv, B. Alonso, J. Durand, B. Bujoli, Z. Gan, G. Hoatson, Modelling one- and two-dimensional solid-state NMR, (2002) 70–76. doi:10.1002/mrc.984.

[37] NF EN 12457-2 December 2002, Leaching — Compliance test for leachingof granular waste materials and sludgesPart 2: One stage batch test at a liquid to solid ratio of 10 l/kgfor materials with particle size below 4 mm (without or with size reduction), (n.d.).

[38] N.E. 196-1 (septembre 2016), Methods of testing cement — Part 1: Determination of strength, (n.d.).

[39] A. Bouchikhi, M. Benzerzour, N.-E. Abriak, W. Maherzi, Y. Mamindy-Pajany, Study of the impact of waste glasses types on pozzolanic activity of cementitious matrix, Constr. Build. Mater. 197 (2019) 626–640. doi:10.1016/j.conbuildmat.2018.11.180.

[40] N. Billong, L. Boubakar, B.N. Bayiha, S.M. Njimbouombouo, U.C. Melo, J. Oti, J. Kinuthia, An investigation on the suitability of hydrated building lime from travertine limestone outcrop of Bogongo, South West of Cameroon, Case Stud. Constr. Mater. 13 (2020) e00369. doi:10.1016/j.cscm.2020.e00369.

[41] R. Idir, M. Cyr, A. Tagnit-Hamou, Pozzolanic properties of fine and coarse color-mixed glass cullet, Cem. Concr. Compos. 33 (2011) 19–29. doi:10.1016/j.cemconcomp.2010.09.013.

[42] R. Idir, M. Cyr, A. Tagnit-Hamou, Use of fine glass as ASR inhibitor in glass aggregate mortars, Constr. Build. Mater. 24 (2010) 1309–1312. doi:10.1016/j.conbuildmat.2009.12.030.

[43] R.IDIR, Mecanismes d'action des fines et des granulats de verre sur la reaction alcali-silice et la reaction pouzzolanique, SHERBROOKE, 2011.

[44] A. Al-Sibahy, R. Edwards, Mechanical and thermal properties of novel lightweight concrete mixtures containing recycled glass and metakaolin, Constr. Build. Mater. 31 (2012) 157–167. doi:10.1016/j.conbuildmat.2011.12.095.

[45] R. Dron, F. Brivot, Thermodynamic and Kinetic Approach To the Alkali- Silica Reaction. Part

2: Experiment, Cem. Concr. Res. 23 (1993) 93–103.

[46] V. Vaitkevičius, E. Šerelis, H. Hilbig, The effect of glass powder on the microstructure of ultra high performance concrete, Constr. Build. Mater. 68 (2014) 102–109. doi:10.1016/j.conbuildmat.2014.05.101.

[47] J. 2014, F. n°0289 D. 14th, Ministerial decree12 Decembre 2014, Off. Page French Gov. (2014) 21032 Texte 11.

[48] F. Gervais, A. Blin, D. Massiot, J.P. Coutures, M.H. Chopinet, F. Naudin, Infrared reflectivity spectroscopy of silicate glasses, J. Non. Cryst. Solids. 89 (1987) 384–401. doi:10.1016/S0022-3093(87)80280-6.

[49] B.O. Mysen, J.D. Frantz, Structural studies of silicate glasses and melts-applications and limitations of Raman spectroscopy, Contrib. to Mineral. Petrol. 117 (1994) 1–14. doi:10.1007/BF00307725.

[50] S.A. Bernal, J.L. Provis, D.G. Brice, A. Kilcullen, P. Duxson, J.S.J. Van Deventer, Accelerated carbonation testing of alkali-activated binders significantly underestimates service life: The role of pore solution chemistry, Cem. Concr. Res. 42 (2012) 1317–1326. doi:10.1016/j.cemconres.2012.07.002.

[51] J. Temuujin, C. Ruescher, A. Minjigmaa, B. Darkhijav, B. Davaabal, B.E. Battsetseg, Characterization of Effloresences of Ambient and Elevated Temperature Cured Fly Ash Based Geopolymer Type Concretes, Adv. Mater. Res. 1139 (2016) 25–29. doi:10.4028/www.scientific.net/amr.1139.25.

[52] S.E. Lappi, B. Smith, S. Franzen, Infrared spectra of H216O, H218O and D2O in the liquid phase by single-pass attenuated total internal reflection spectroscopy, Spectrochim. Acta - Part A Mol. Biomol. Spectrosc. 60 (2004) 2611–2619. doi:10.1016/j.saa.2003.12.042.

[53] S. Onisei, A.P. Douvalis, A. Malfliet, A. Peys, Y. Pontikes, Inorganic polymers made of fayalite slag: On the microstructure and behavior of Fe, J. Am. Ceram. Soc. 101 (2018) 2245–2257. doi:10.1111/jace.15420.

[54] A.. Poole, Alkali-Silica reactivity mechanisms of gel formation and expansion, Proceedings of the 9th International Conference on Alkali-Aggregate Reaction, London (England), 104 (1), Concrete Society Publications CS, pp. 782-789, 1992, London (England), 104 (1), Concr. Soc. Publ. CS. (1992) London (England), 104 (1), Concrete Society Public.

[55] N. Koshy, D.N. Singh, Fly ash zeolites for water treatment applications, Biochem. Pharmacol.

4 (2016) 1460–1472. doi:10.1016/j.jece.2016.02.002.

[56] Q.Y. Chen, M. Tyrer, C.D. Hills, X.M. Yang, P. Carey, Immobilisation of heavy metal in cement-based solidification/stabilisation: A review, Waste Manag. (2009). doi:10.1016/j.wasman.2008.01.019.

[57] H. Xu, J.S.J. Van Deventer, G.C. Lukey, Effect of alkali metals on the preferential geopolymerization of stilbite/kaolinite mixtures, Ind. Eng. Chem. Res. 40 (2001) 3749–3756. doi:10.1021/ie010042b.

[58] T. Deschamps, M. Benzaazoua, B. Bussière, T. Belem, M. Mbonimpa, Mécanismes de rétention des métaux lourds en phase solide : cas de la stabilisation des sols contaminés et des déchets industriels, VertigO. 7 (2006) 0–11. doi:10.4000/vertigo.2171.

[59] B.I. El-Eswed, R.I. Yousef, M. Alshaaer, I. Hamadneh, S.I. Al-Gharabli, F. Khalili, Stabilization/solidification of heavy metals in kaolin/zeolite based geopolymers, Int. J. Miner. Process. 137 (2015) 34–42. doi:10.1016/j.minpro.2015.03.002.

[60] T.W. Cheng, M.L. Lee, M.S. Ko, T.H. Ueng, S.F. Yang, The heavy metal adsorption characteristics on metakaolin-based geopolymer, 56 (2012) 90–96. doi:10.1016/j.clay.2011.11.027.

[61] İ. Kara, D. Yilmazer, S. Tunali, Metakaolin based geopolymer as an effective adsorbent for adsorption of zinc (II) and nickel (II) ions from aqueous solutions, Appl. Clay Sci. 139 (2017) 54–63. doi:10.1016/j.clay.2017.01.008.

[62] E. Papa, V. Medri, S. Amari, J. Manaud, P. Benito, A. Vaccari, E. Landi, Zeolite-geopolymer composite materials: Production and characterization, J. Clean. Prod. 171 (2018) 76–84. doi:10.1016/j.jclepro.2017.09.270.

[63] B.V. and R.H. N. Alharbi, Alkali-activated slag characterization by scanning Electron microscopy, X-ray microanalysis and nuclear magnetic resonance spectroscopy, Sensors Actuators B. Chem. (2019) 127065. doi:10.1016/j.snb.2019.127065.

[64] N.B. Singh, Fly ash-based geopolymer binder: A future construction material, Minerals. 8 (2018). doi:10.3390/min8070299.